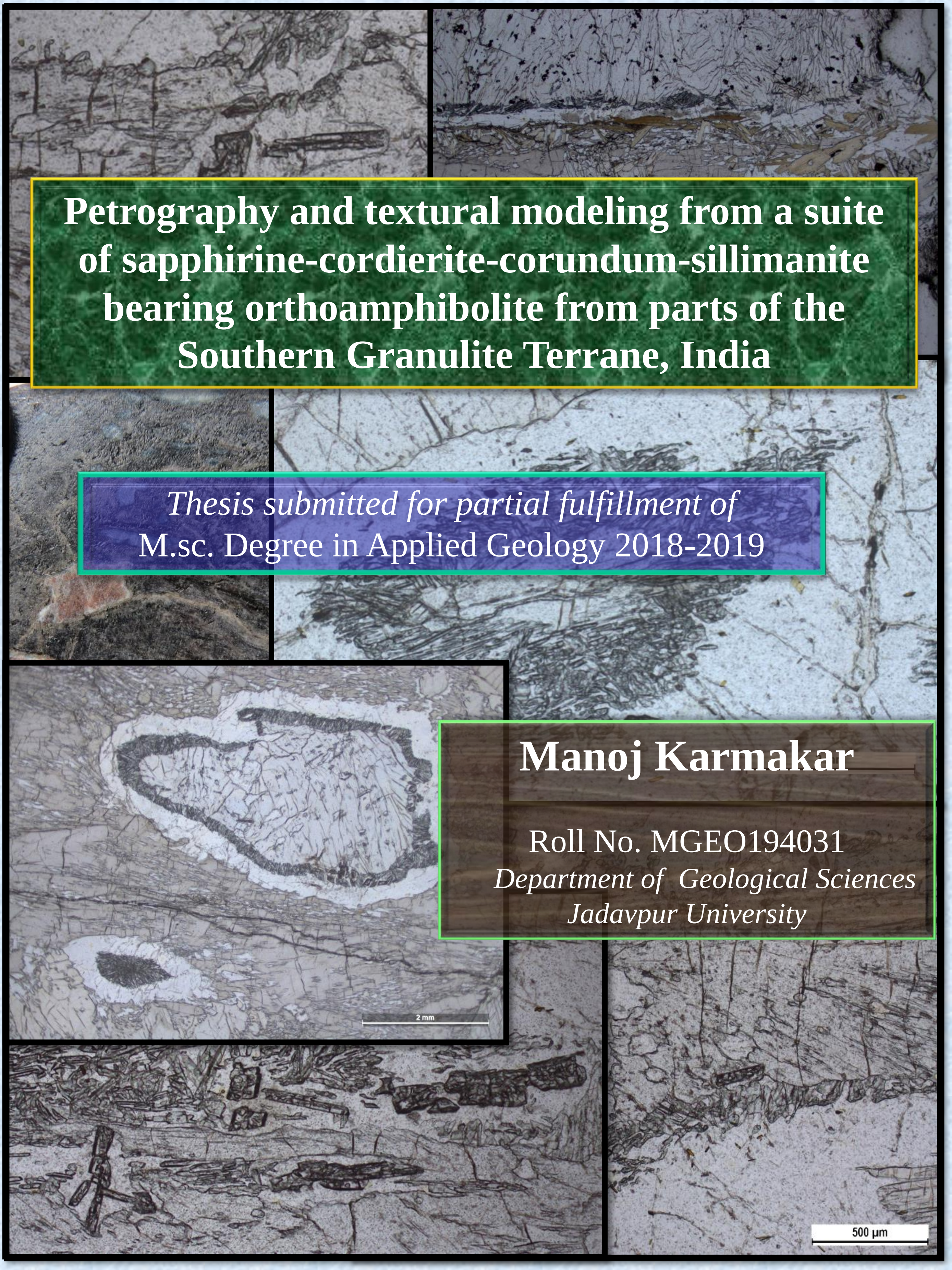

Petrography and textural modeling from a suite of sapphirine-cordierite-corundum-sillimanite bearing orthoamphibolite from parts of the Southern Granulite Terrane, India

Thesis submitted for partial fulfillment of
M.sc. Degree in Applied Geology 2018-2019

Manoj Karmakar

Roll No. MGEO194031
Department of Geological Sciences
Jadavpur University

Petrography and textural modeling from a suite of sapphirine-cordierite-corundum-sillimanite bearing orthoamphibolite from parts of the Southern Granulite Terrane, India

Thesis submitted for partial fulfillment of
M.Sc. Degree in Applied Geology
2018-2019

Manoj Karmakar

Roll No. **MGEO194031**
Registration No. **142791 of 2017-2018**

Department of Geological Sciences
Jadavpur University

যাদবপুর বিশ্ববিদ্যালয়
কলকাতা-৭০০০৩২, ভারত

JADAVPUR UNIVERSITY
KOLKATA-700032, INDIA

FACULTY OF SCIENCE : DEPARTMENT OF GEOLOGICAL SCIENCES

CERTIFICATE FROM THE SUPERVISOR

This is to certify that **Mr. Manoj Karmakar** has worked under the supervision of Prof. Subrata Karmakar in the Department of Geological Sciences, Jadavpur University and completed his thesis entitled **"Petrography and textural modeling from a suite of sapphirine-cordierite-corundum-sillimanite bearing orthoamphibolite from parts of the Southern granulite Terrane, india"** which is being submitted towards the partial fulfillment of his M.Sc. Final Examination in Applied Geology of Jadavpur University in 2019.

Signature of the Supervisor:

Subrata Karmakar
30/05/19

Prof. Subrata Karmakar
Dept. of Geological Sciences
Jadavpur University

Dr. Subrata Karmakar
Professor
Department of Geological Sciences
Jadavpur University
Kolkata: 700032, India

Signature of Head of the Department:

Sanjoy Sanyal
31/05/2019

Prof. Sanjoy Sanyal
Dept. of Geological Sciences
Jadavpur University

Head
Department of Geological Sciences
Jadavpur University
Kolkata-700032

দূরভাষ : ২৪১৪-৬৬৬৬/প্রসারণ : ২২৬৮
Website : www.jadavpur.edu
E-mail : hod_geological@jdvu.ac.in
Phone : 2414 6666/Extn. 2268

Contents

Abstract

The Granulitic Terrane of South India exposes diverse variety of late mafic and ultramafic enclaves, hosted within late Archaean felsic orthogneiss. These Archean rocks are dissected by a number of crustal scale shear zones collectively named as Cauvery Shear System (CSS). The eastern part of CSS exposes intensely deformed mafic and felsic granulites that are extensively altered to amphibolite facies ensembles. This study focuses on one of such highly retrogressed rock-units near Sevitthurangampatti that is dominated by ortho-amphibole (gedrite) ± kyanite/sillimanite and contains rare and exotic mineral assemblages of sapphirine+cordierite+corundum. Microscopic study reveals that symplectic intergrowth of these three minerals forms corona and pseudomorphs over sillimanite. Petrographic study aided with mineral chemical analysis suggests a two stage reaction that led to the formation of sapphirine-cordierite symplectite and corundum-cordierite successively, at the expense of gedrite and sillimanite.

Textural modeling of the pseudomorph and corona suggest the following balanced reactions with several mobile elements like Mg, Fe, Na and SiO_2 *were responsible for the formation of these assemblages.*

(1) 5.80 Gedrite + 30.69 Sillimanite + 3.32 Mg^{2+} = 2.04 Sapphirine + 13.67 Cordierite + 1.00 Na^{+} + 2.30 Fe^{2+} + 5.80 H_2O

(2) 130.10 Sillimanite + 12.38 Sapphirine + 1.00 Na^{+}+ = 147.30 Corundum + 20.00 Cordierite + 48.09 SiO_2 + 1.09 Fe^{2+}

Brine-rich aqueous fluids can potentially play an important role in this element transfer process. Calculation of petrogenetic grid in MASH system constrains a decompressive P-T path from 760-880°C and 6.5-8.5 kbar. At least a part of the CSS experienced infiltration-induced retrogression at granulite grade conditions during the Pan-African time.

1. Introduction:

Frozen-in textures such as coronas, symplectites and pseudomorphs attract the interest of petrologists because of their distinct appearance. Presence of these textures in rock provides precious clues for understanding the element behavior (mass transfer, diffusion, kinetic controls etc.) during their formation (Chowdhury et al., 2013; Putnis 2002; Putnis et al., 2005; Philpotts and Ague 2009; Ague 2011 and others). Moreover, these disequilibrium textures often act as excellent guides for reaction relations and chronology between different minerals which can be successfully utilized to constrain metamorphic pressure (P)–temperature (T) paths in orogenic belts (e.g., Nishiyama, 1983; Ashworth and Birdi, 1990; Nakamura, 2002; Santosh and Sajeev, 2006).

Orthoamphibole-cordierite-sapphirine±corundum gneisses have been reported from many terranes worldwide (Kelsey et al., 2005). These rocks constitute a special segment of Mg-Al rocks because of their unusual bulk compositions that do not correspond to typical igneous or sedimentary protoliths (e.g. Eskola, 1914; Chinner & Fox, 1974; Robinson et al., 1982). Their bulk compositions may be attributed to modification by severe infiltration-metasomatism, partial melting or interaction with melt, or polyphase histories (e.g. Tilley, 1937; Vallance, 1967; Schumacher, 1988; Pan & Fleet, 1995; Peck & Smith, 2005; Raith et al., 2008 and references therein). Nevertheless, because of these unusual bulk compositions, these rocks commonly display various disequilibrium textures (e.g coronas and symplectites) that provide clues about metamorphic history, and therefore tectonic processes(Robinson & Jaffe, 1969; James et al., 1978; Robinson et al., 1982; Schumacher & Robinson 1987; Schneiderman & Tracy, 1991; Diener et al., 2008 and references there in).

In this study, I document coronal and pseudomorphic replacement textures defined by sapphirine-cordierite±corundum symplectites in a sillimanite bearing orthoamphibolite(orthoamphibole-dominated) rock from parts of the Southern Granulitic terrane, India. Petrographic study aided with mineral chemical analysis suggests a two stage reaction that led to the successive formation of sapphirine-cordierite symplectite followed by corundum-cordierite. Textural modeling of the pseudomorph and corona suggest that several elements were mobile during their formations. Calculation of petrogenetic grid constrains the retrogressive P-T path of the terrane during the Pan-African time.

2. Geological background:

The Southern Granulitic Terrane (SGT) of India comprises a collage of poly-metamorphic terrains that experienced a protracted crustal evolution history ranging from Early Archaean to late Neoproterozoic (Harris et al., 1994; Bartlett et al., 1998; Braun and Kriegsman, 2003; Santosh et al., 2003, 2005).On the basis of the extant geological and geochronological information, the SGT can be divided into three roughly east–west elongated units, namely, the Northern granulite block, the Cauvery shear system and the Madurai block(Fig.1), which all have distinct geological histories (reviewed by Braun & Kriegsman, 2003;Ghosh et al., 2004; Plavsa et al., 2012; Brandt et al.,2014).(Fig.1).

The felsic orthogenesis dominated Northern granulite block (NGB) is juxtaposed against the Archaean Dharwar Craton and records signatures of late Archaean(2.7–2.5 Ga) arc magmatism as well as an early Palaeoproterozoic (2.49–2.44 Ga) high grade metamorphism, The southern Madurai block (MB) is dominated by supracrustals which were deposited on a Neoarchaean - Palaeoproterozoic basement and metamorphosed by Pan-African (~0.45-0.65 Ga) granulite grade event. A central zone named Cauvery Shear System (CSS) separates the NGB from MB and exposes a plethora of rocks having diverse bulk compositions and metamorphic grade. They preserve records of crustal evolution from ~2.9Ga to 0.5Ga. A set of extensive east–west striking lithosphere-scale shear zone are presumed to have affected the rocks of the CSS.

Our study area is from the CSS. In view of that we present below the salient points regarding the evolution of this belt. The oldest lithology of the CSS includes a suite of mafic and ultramafic rocks with minor anorthosite and chromitite layers intercalated with BIF units, as enclaves within the surrounding felsic orthogneisses. Extant geochemical, petrological and geochronological studies suggest that these enclaves are remnants of Archean (~3.0-2.5 Ga) oceanic crust (Ghosh et. al., 2004; Dutta et al., 2011;Santosh et al., 2013) that was intruded by voluminous felsic magmas (now ortho-gneisses) with a Neoarchean emplacement age (2.54–2.50 Ga; reviewed by Ghosh et al., 2004; Yellappa et al., 2012; Santosh et al., 2013).Subsequently, the mafic–ultramafic–BIF packages and felsic rocks together underwent deformation and high-grade metamorphism from 2.48 to 2.43 Ga (Ghosh et al., 2004; Yellappa et al., 2012; Santosh et al., 2013; Brandt et al., 2014; Chowdhury and Chakrabarti 2016). This late Archaean to early Paleoproterozoic, high-grade rock ensemble of the CSS remained largely undisturbed for a prolonged period until the onset of Pan-African tectonothermal events (c. 0.72–0.5 Ga: Meißner et al.,2002; reviewed by Ghosh et al., 2004).

Many studies reported occurrences of ultrahigh-temperature Mg–Al granulites, from both NGB and within the CSS that occur as enclaves of variable thickness within felsic ortho-gneiss host rocks. In most of these localities, sapphirine occurs in association with ortho-amphibole(gedrite) + sillimanite + cordierite + corundum.

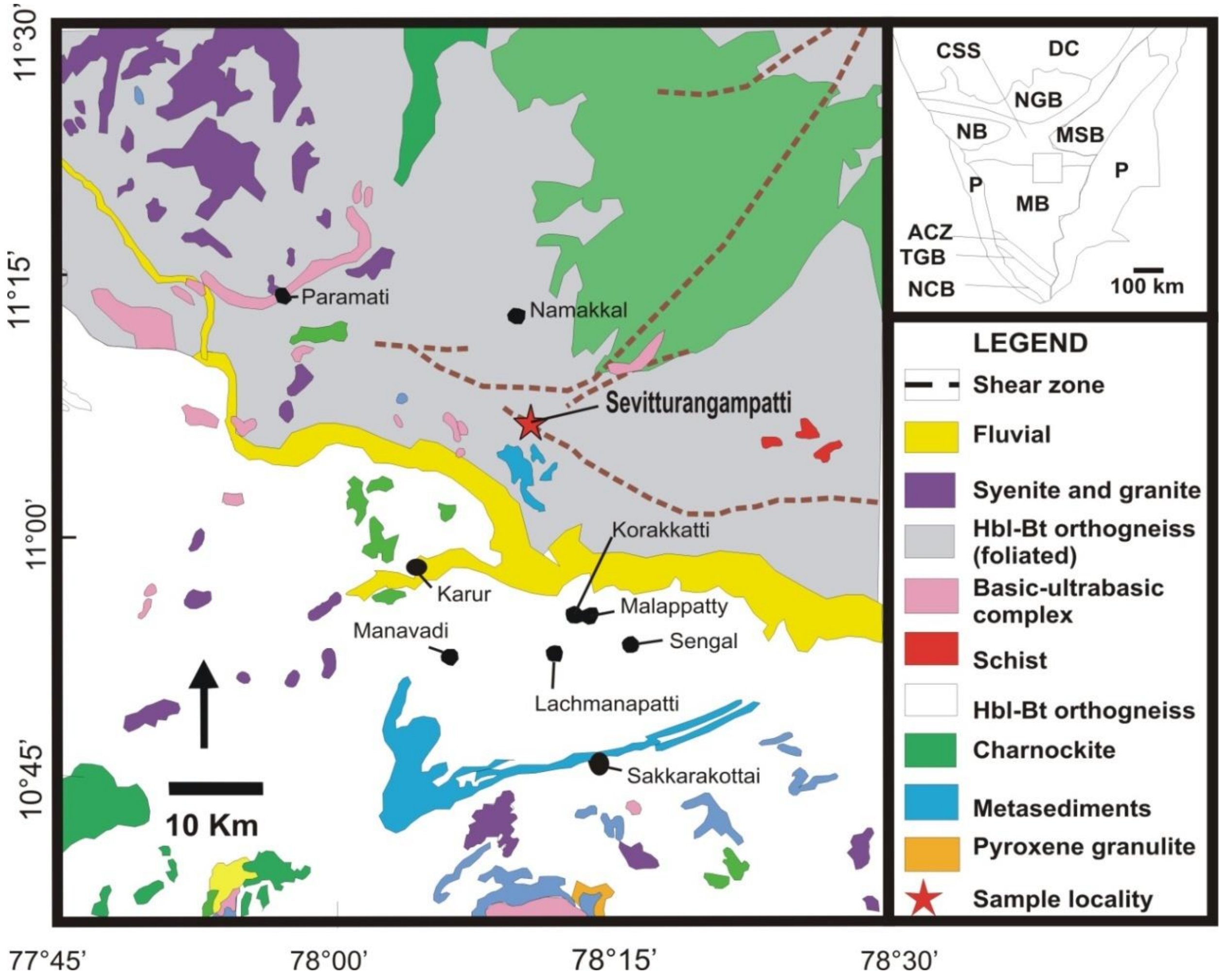

Fig. 1. Geological map of the northern Madurai Block and the Cauvery Shear Zone System (based on 1:500,000 map of Tamil NaduGSI (Geol. Surv. India), Geological and mineral map of TamilNadu and Pondicherry, 1995.)with the sample locality of gedrite-sillimanite-sapphirine-cordierite- corundum bearing mafic enclaves within the felsic ortho-gneisses discussed in this paper. DC: Dharwar Craton, MB: Madurai Block, MSB: Madras Block, NGB: Northern Granulite Block, NB: Nilgiri Block, TGB: Trivandrum Granulite Block, NCB: Nagarcoil Block, ACZ: Achankovil Shear Zones, CSS: Cauvery Shear Zone System, P: Phanerozoic cover(modified after M. Shimpo et al. 2006).

These include Savitthurangampatti (Shimpo et al. 2006), Perumalmalai (Brown and Raith, 1996; Raith et al.,1997),Panrimalai (Grew;1984),Lachmanapatti and Malappatty (Tsunogae and Santosh, 2003), Paramati (Koshimoto et al., 2004; Santosh et al., 2004), Sengal and Sakkarakottai (Santosh and Sajeev 2004;

Tamashiro et al 2004), Manavadi and Korakkatti (Koshimoto et al. 2004; Tsunogae and Santosh 2003) (Fig.1). U–Pb ages of zircon and monazite in a few of these rocks suggest that the UHT metamorphism occurred during Pan-African time(c. 600–500 Ma, Santosh et. al., 2006). But as sapphirine in equilibrium with quartz has not been identified so far from this area, >1000°C temperature reported by the authors have remained elusive. In view of that, this study intends to constrain the P-T conditions of formation of sapphirine-corundum-cordierite assemblage from such a Mg-Al granulite rock near Sevitthurangampatti in CSS (Fig.1).

2.1 Field occurrence:

The study area, Sevitthurangampatti village is located at about 13 km south of the Namakkal town in Tamil Nadu. The lithologic units of region or the host rock lithology comprise felsic ortho-gneiss with some mafic enclaves (Fig 2A, 2B & 2C). At Sevitthurangampatti, extensive pits dug into the bedrock expose patches of highly retrogressed hydrous mineral (biotite-gedrite) rich gneissic rocks with some exotic minerals like corundum, sapphirine, cordierite and sillimenite and gedrite.

In hand specimen, the sample is melanocratic, dark grey coloured, coarse grained and dominantly composed of two minerals namely gedrite and sillimanite. Large gedrite grains(upto 6 cm) are long prismatic, dark grey and are randomly oriented (Fig 2D). Sillimanite grains are white coloured, accicular, 3-4cm long and are always present in between the gedrite grains. In cross sectional plane of the rock, small micro-domains (0.5-2.0 cm) that contains minerals like Sillimanite, sapphirine, cordierite are visible (Fig 2E).

Tabular grains of sillimanite are always rimmed by a blue colored corona composed of sapphirine and/or cordierite (Fig 2E). In places, in absence of sillimanite, sapphirine and cordierite together constitute the oval shaped micro domains (Fig 2E).

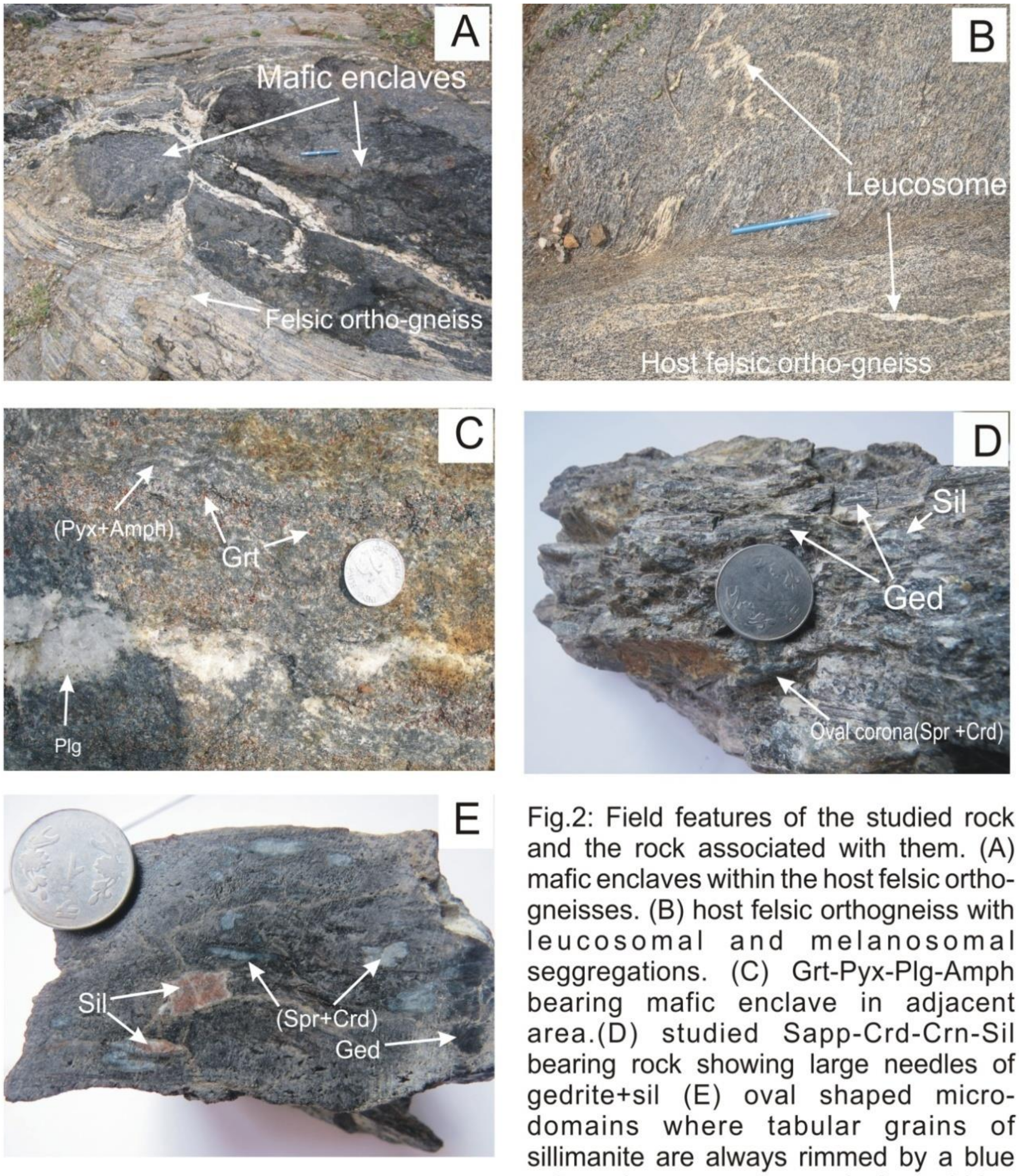

Fig.2: Field features of the studied rock and the rock associated with them. (A) mafic enclaves within the host felsic ortho-gneisses. (B) host felsic orthogneiss with leucosomal and melanosomal seggregations. (C) Grt-Pyx-Plg-Amph bearing mafic enclave in adjacent area.(D) studied Sapp-Crd-Crn-Sil bearing rock showing large needles of gedrite+sil (E) oval shaped micro-domains where tabular grains of sillimanite are always rimmed by a blue coloured corona composed of sapphirine and/or cordierite.

3. Petrography:

This subsection presents mutual relationship between different minerals in the studied rock under microscope. Gedrite 38%, sapphirine 14%, sillimanite 22%, cordierite 24%, corundum 1% and rutile 2% are the major constituting minerals.

Large needles of gedrite are hapazardly dispersed throughout the section (fig-3A). Gedrite is the most dominant mineral and form the groundmass in the rock. Individual gedrite grains are generally 4-6mm in size and are closely packed with each other (fig-3B). They are randomly oriented without having any particular directional orientation. Sillimanite grains are dispersed randomly within the gedrite-dominated mass. Intriguingly, sillimanite have tabular shapes suggesting that these grains could be kyanite pseudomorph.

Within this bi-mineralic groundmass, there occur few micro-domains that contain sillimanite, sapphirine, cordierite, and corundum (fig-3C). These minerals exhibit distinct disequilibrium textures. Sillimanite is always separated from gedrite by a double corona of sapphirine-corundum-cordierite symplectite and cordierite. The symplectic intergrowth occurs adjacent to sillimanite while the cordierite occurs adjacent to gedrite (fig-3D & 3E). The sapphirine needles in the symplectic corona are colourless, each ranges from 0.3-0.4mm in size and are haphazardly distributed along the corona within a mass of cordierite. The ratio of cordierite and sapphirine in the symplectic corona is about 1:2.5 to 1:3. Corundum is unevenly distributed with the symplectite. But they always occur just adjacent to the sillimanite grain boundary. The presence of corundum in symplectic corona is usually associated with an absence of sapphirine in its surrounding (over a zone 2-3 times larger than the volume of the respective corundum) and an embayment in the adjacent sillimanite grain (fig-3F).

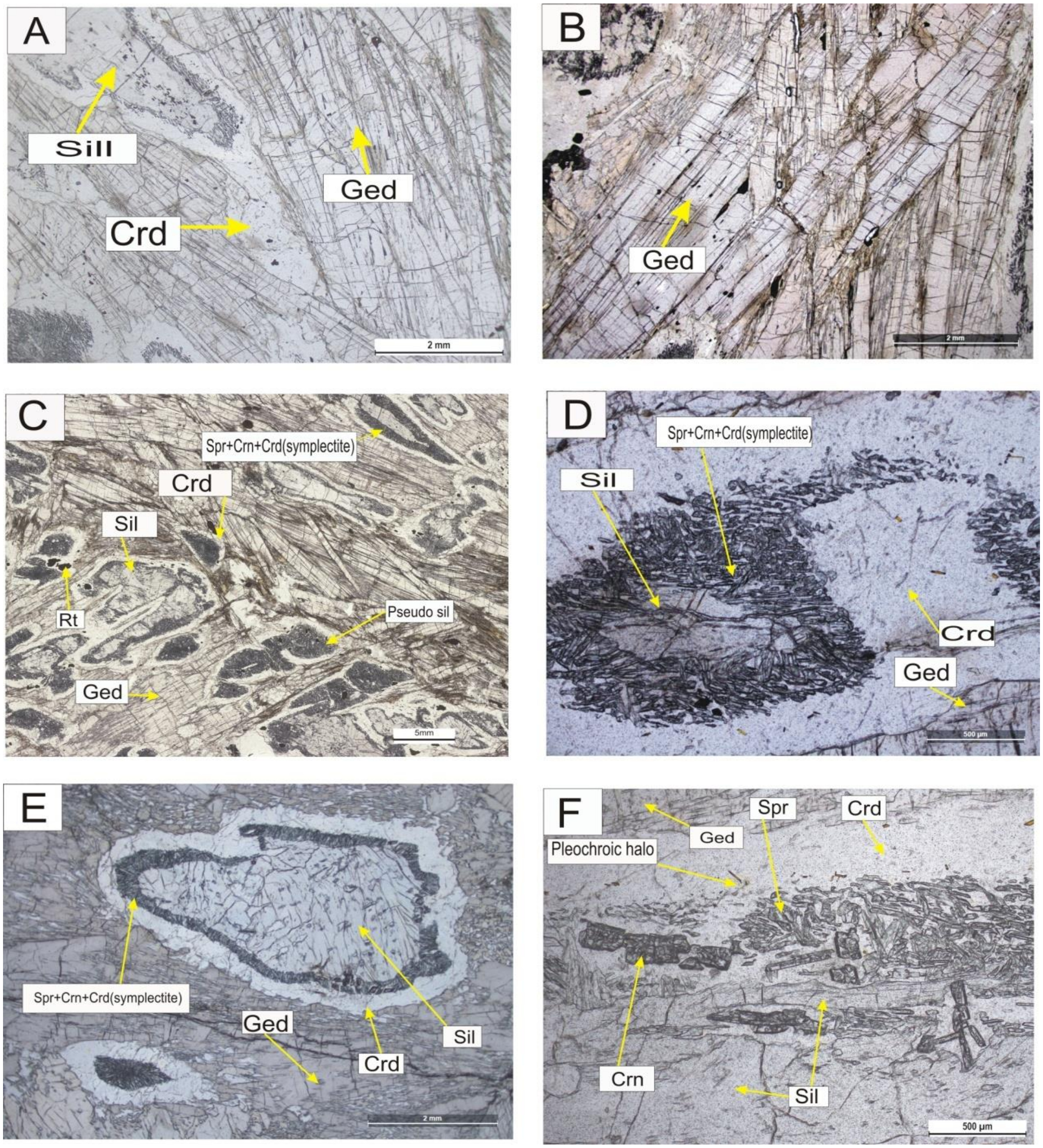

Fig. 3: Photomicrographs showing the different microtextural features of the studied rock. Abbreviation of mineral names after Kretz (1983) (A) Haphazardly distributed large blades of sillimanite and needles of gedrite.(B) Large gedrite grains closely packed with each other.(C) Few micro-domains that contain sillimanite, sapphirine, cordierite, and corundum within the monomineralic gedrite-dominated groundmass. (D) & (E) Symplectic intergrowth of sapphirine, cordierite and corundum over sillimanite with a collar of cordierite around it, separating sillimanite from gedrite. Note the size of the relict sillimanite within the symplectic corona varies and shows a negative correlation with the thickness of the symplectic corona.(F) corundum and cordierite forming embayment within adjacent sillimanite grains.

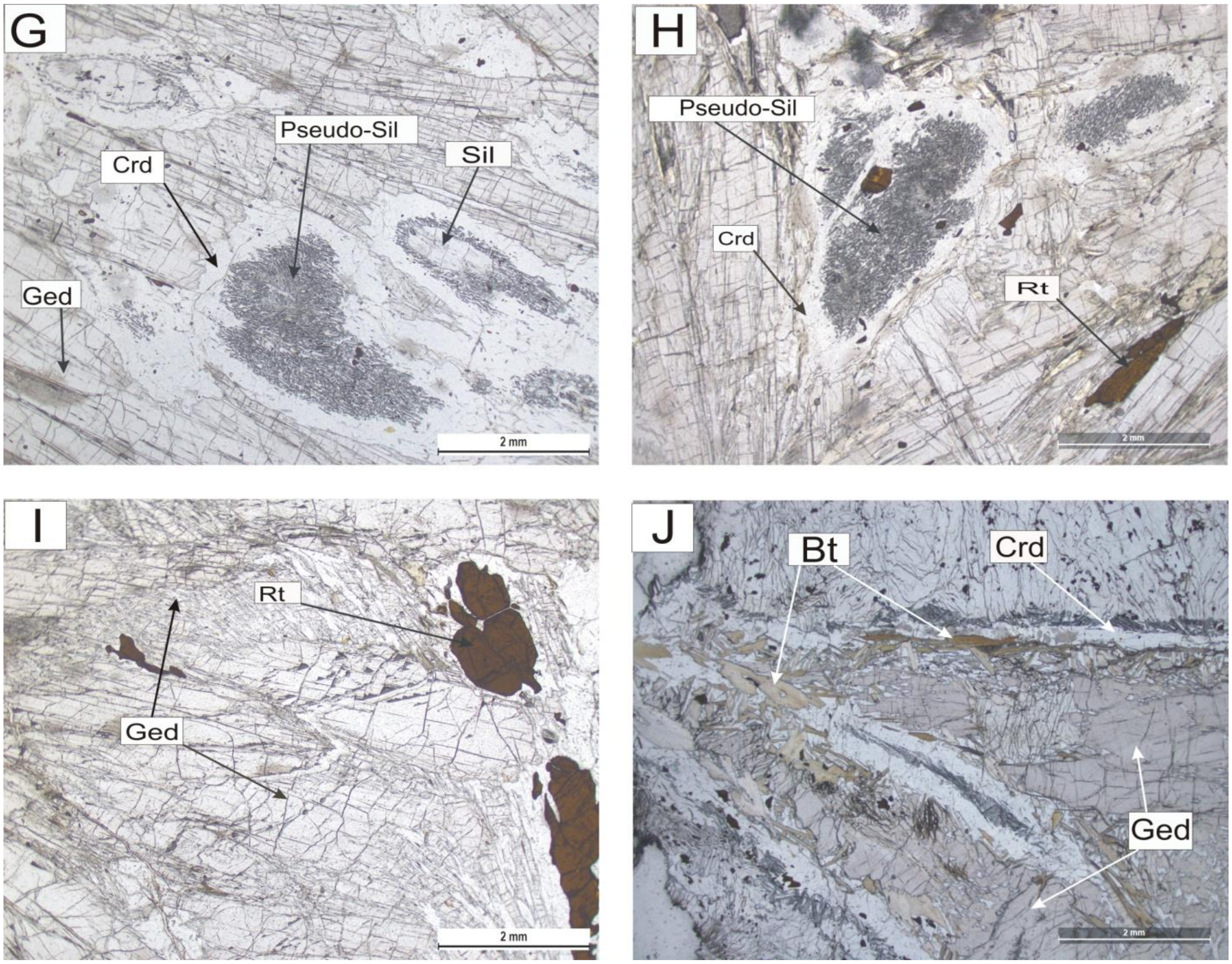

Fig. 3.continued: Photomicrographs showing the different microtextural features of the studied rock. (G) & (H) Micro domains where the sillimanite grains are completely pseudomorphed by the sapphirine-cordierite symplectite. (I) Medium to large sized rutile grains dispersed within the gedrite rich groundmass. (J) biotite grains developed along the contact boundaries of cordierite and gedrite.

As the volume fraction of sapphirine in the symplectic assemblage is more or less constant, the volume ratio of corundum and the sapphirine which is absent from its surrounding region within symplectite can be predicted to be around 1:1 to 1:1.5. The size of the relict sillimanite within the symplectic corona varies from one micro-domain to other and shows a negative correlation with the thickness of the symplectic corona (fig-3D, 3E, 3G).

Rarely in few micro domains, the sillimanite grains are completely pseudomorphed by the sapphirine-cordierite symplectite (fig-3G, 3H). Corundum is absent in those pseudomorphs which are completely lack of relict sillimanite. The rutile grains are mediumto large in size (upto 1.5mm) and are dispersed within the gedrite-rich groundmass (fig-3I). At Few places rutile grain occur as an embayment within a large sillimanite grains. Rarely quartz is present within gedrite as inclusions. At very few places biotite grains has developed along the contact boundaries of cordierite and gedrite (fig-3J).

4. Mineral chemistry:

Analytical techniques:

All mineral analyses for the studied rock were performed with a Cameca SX100 Electron Probe Micro Analyzer (EPMA) at the Department of Geology and Geophysics, Indian Institute of Technology, Kharagpur. All points were analyzed with an accelerating voltage of 15 kV, a beam current of 20 nA and a beam size of 1 µm. Dwell time for the measured elements was set at 10 s for peak and 5 s for background. The ZAF correction scheme was used. Both natural and synthetic samples were used for standards. During cation recalculation from oxide weight percentage, Fe^{+3} is calculated after the scheme of Droop, 1987. Representative data of minerals are presented in Table 1a and 1b. The compositional data are provided to me by Dr. Anindita Dey (her unpublished data).

Sapphirine: The sapphirine is highly magnesian with X_{Mg} = 0.94- 0.95 apfu. The Fe^{3+}/Fe^{2+} ratio of sapphirine as recalculated from the charge balance method range is between 0.6 and 1.1apfu. No significant difference was noted between compositions of different sapphirine grains. The $Al/(Al + Fe)^{3+}$ ratio is restricted at

0.99. When plotted in the $(Al + Fe)^{3+}$ vs. $(Si + Mg + Fe^{2+})$ diagram, sapphirine compositions show a linear spread connecting 7:9:3 and 3:5:1 sapphirine structure (fig. 4A).

Table 1a. Representative oxide analysis and calculated cations of sapphirine and Cordierite.

	Sapphirine					Cordierite				
point No.	26 / 1 . *	27 / 1.	28 / 1.	29 / 1.	32 / 1 .	25 / 1 . *	34 / 1.	35 / 1.	39 / 1.	43 / 1.
SiO_2	11.149	11.255	11.340	11.263	11.749	50.226	50.125	36.951	50.378	50.095
TiO_2	0.013	0.005	0.000	0.014	0.002	0.000	0.000	0.019	0.000	0.022
Al_2O_3	67.229	67.011	65.555	66.604	66.723	33.385	33.298	61.875	33.272	33.104
Cr_2O_3	0.260	0.463	0.943	0.449	0.550	0.000	0.000	0.236	0.000	0.000
FeO	2.608	2.878	2.914	2.757	2.841	1.207	1.087	0.000	1.022	1.193
MnO	0.000	0.000	0.052	0.000	0.136	0.000	0.117	0.000	0.000	0.000
MgO	18.099	18.005	18.149	18.109	18.408	13.228	13.132	0.004	13.306	13.059
ZnO	0.000	0.067	0.086	0.122	0.213	0.168	0.000	0.000	0.107	0.042
CaO	0.000	0.002	0.002	0.001	0.003	0.031	0.030	0.000	0.023	0.042
Na_2O	0.002	0.013	0.000	0.000	0.000	0.279	0.236	0.000	0.316	0.228
K_2O	0.000	0.000	0.006	0.000	0.002	0.007	0.000	0.000	0.000	0.022
Total	99.360	99.699	99.047	99.345	100.650	98.531	98.055	99.085	98.424	97.807
cation basis	14	14	14	14	14	11	11	11	11	11
oxygen basis	20	20	20	20	20	18	18	18	18	18
Si (apfu)	1.303	1.314	1.335	1.319	1.360	4.977	4.991	3.692	4.992	5.003
Ti	0.001	0.000	0.000	0.001	0.000	0.000	0.000	0.001	0.000	0.002
Al	9.262	9.220	9.093	9.193	9.103	3.899	3.908	7.287	3.886	3.897
Cr	0.024	0.043	0.088	0.042	0.050	0.000	0.000	0.019	0.000	0.000
Fe^{+3}	0.105	0.112	0.151	0.122	0.124	0.100	0.091	0.000	0.085	0.100
Fe^{+2}	0.150	0.169	0.136	0.148	0.151	0.000	0.000	0.000	0.000	0.000
Mn	0.000	0.000	0.005	0.000	0.013	0.000	0.010	0.000	0.000	0.000
Mg	3.154	3.133	3.184	3.162	3.177	1.954	1.949	0.001	1.966	1.944
Zn	0.000	0.006	0.007	0.011	0.018	0.012	0.000	0.000	0.008	0.003
Ca	0.000	0.000	0.000	0.000	0.000	0.003	0.003	0.000	0.002	0.004
Na	0.000	0.003	0.000	0.000	0.000	0.054	0.046	0.000	0.061	0.044
K	0.000	0.000	0.001	0.000	0.000	0.001	0.000	0.000	0.000	0.003
Total	14	14	14	14	14	11	11	11	11	11
XMg	0.955	0.949	0.959	0.955	0.955	1.00	1.00	1.00	1.00	1.00
$(Al+Fe)^{3+}$	9.368	9.332	9.244	9.315	9.227	3.998	3.998	7.286	3.97	3.996
$Fe^{3+}/(Al+Fe)^{3+}$	0.011	0.012	0.016	0.013	0.013	0.025	0.023	0.000	0.021	0.025

*data used for compositional modeling

Table 1b. Representative oxide analysis and calculated cations of Gedrite, Corundum and Sillimanite.

	Gedrite					Corundum	sillimanite	
point no.	24 / 1 . *	36 / 1 .	40 / 1 .	41 / 1 .	42 / 1 .	31 / 1 .*	30 / 1 . *	33 / 1.
SiO_2	50.626	50.742	49.087	48.984	50.114	0.021	37.282	36.941
TiO_2	0.276	0.213	0.36	0.322	0.307	0.000	0.000	0.000
Al_2O_3	12.701	12.577	14.206	13.885	13.047	98.328	62.008	61.804
Cr_2O_3	0.109	0.087	0.133	0.059	0.013	0.219	0.057	0.000
FeO	6.43	7.208	7.784	7.203	7.676	0.134	0.305	0.094
MnO	0.135	0.000	0.027	0.000	0.109	0.035	0.018	0.027
MgO	25.549	25.795	24.919	24.663	25.329	0.008	0.009	0.038
ZnO	0.000	0.000	0.000	0.000	0.000	0.000	0.000	0.000
CaO	0.383	0.386	0.417	0.435	0.409	0.000	0.005	0.000
Na_2O	1.119	1.108	1.447	1.336	1.228	0.000	0.000	0.001
K_2O	0.000	0.000	0.000	0.000	0.001	0.006	0.023	0.000
Total	97.328	98.116	98.38	96.887	98.233	98.751	99.747	98.905
cation basis	16	16	16	16	16	2	3	3
oxygen basis	23	23	23	23	23	3	5	5
Si(apfu)	6.827	6.803	6.597	6.662	6.730	0.000	1.010	1.008
Ti	0.028	0.021	0.036	0.033	0.031	0.000	0.000	0.000
Al	2.019	1.988	2.251	2.226	2.066	1.994	1.979	1.988
Cr	0.012	0.009	0.014	0.006	0.001	0.003	0.001	0.000
Fe^{+3}	0.332	0.386	0.433	0.406	0.427	0.003	0.000	0.000
Fe^{+2}	0.394	0.423	0.442	0.413	0.435	0.000	0.007	0.006
Mn	0.015	0.000	0.003	0.000	0.012	0.001	0.000	0.001
Mg	5.135	5.154	4.991	4.999	5.070	0.000	0.000	0.002
Zn	0.000	0.000	0.000	0.000	0.000	0.000	0.000	0.000
Ca	0.055	0.055	0.060	0.063	0.059	0.000	0.000	0.000
Na	0.293	0.288	0.377	0.352	0.320	0.000	0.000	0.000
K	0.000	0.000	0.000	0.000	0.000	0.000	0.001	0.000
Total	15.110	15.128	15.206	15.162	15.152	2.000	3.000	3.000
XMg	0.929	0.924	0.919	0.924	0.921	NA	NA	NA
$(Al+Fe)^{3+}$	2.351	2.374	2.684	2.632	2.493	NA	NA	NA
$Fe^{3+}/(Al+Fe)^{3+}$	0.141	0.162	0.161	0.154	0.171	NA	NA	NA

*data used for compositional modeling

Gedrite: The Gedrite is highly magnesian with X_{Mg} = 0.92 to 0.93apfu(fig.4B). Total Fe (Fe^{+2} + Fe^{+3}) vaies from 0.72 to 0.87 apfu with a significant Fe^{+3} content (0.33-0.43 apfu). $(Al + Fe)^{3+}$ varies from 2.35 – 2.68 apfu with $X_{Fe}{}^{3+}$ ($Fe^{3+}/(Al+Fe)^{3+}$) = 0.14 – 0.17. Minor Na (0.29 to 0.35 apfu) and Ca (0.05 to 0.06 apfu) is present. ($Al+Fe^{3+}$) shows positive correlation with Na and negative correlations with Si indicating the replacement $Si^{4+} \rightarrow Na^{+} + (Al+Fe)^{+3}$ (fig. 4C, 4D and 4E).

Cordierite: Cordierite shows restricted compositional range with XMg =1. It contains certain amount of Fe^{+3} (0.08-0.1 apfu) and Na (0.04-0.6 apfu). Moderately high analytical totals (97.8–98.5 wt%) and minor alkali contents in cordierite suggest some amount of channel fluid contents (Armbruster & Bloss 1982).

Sillimenite, Corundum: Sillimanite and corundum shows almost pure composition.

All the ferromagnesian phases are plotted in FAS, MAS and AFM diagram, projected from H_2O (fig. 4E).

In view of the measured compositions of the studied minerals, minerals in descending order of X_{Mg}: cordierite>sapphirine>gedrite; and minerals in descending order of Al: corundum>sapphirine>sillimanite>cordierite>gedrite.

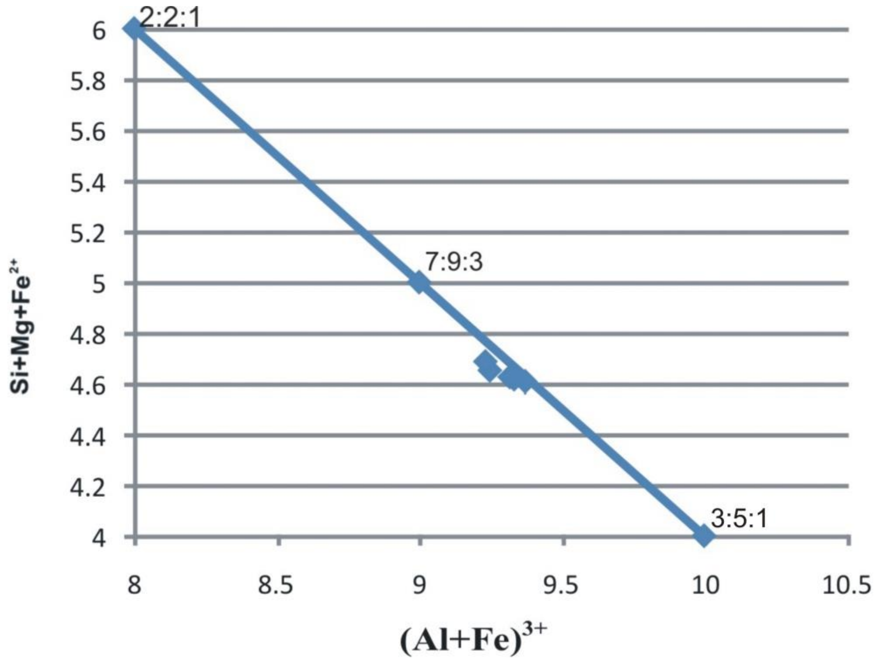

Fig 4a: Compositional variation of sapphirine from the studied area in a plot of (Al+Fe^{3+}) apfu vs. (Si+Mg+Fe^{2+}) apfu showing that the sapphirine composition lie along a linear array in one cluster near the 7:9:3 end member.

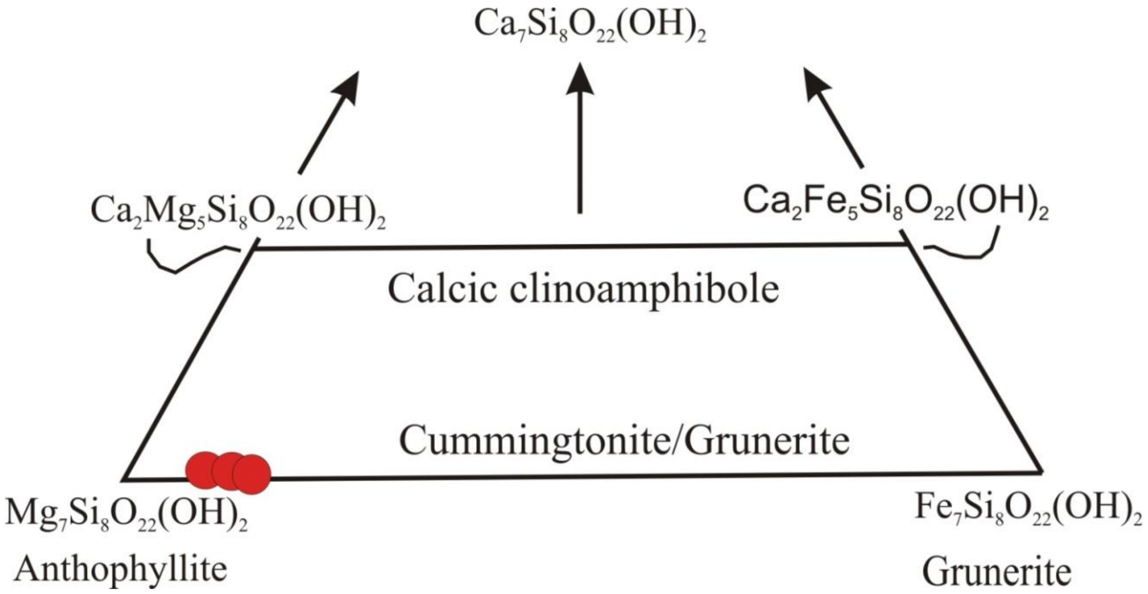

Fig 4b: Composition of the mineral orthoamphibole (gedrite) are shown with red coloure in this triangle of Mg-Fe-Ca amphibole.

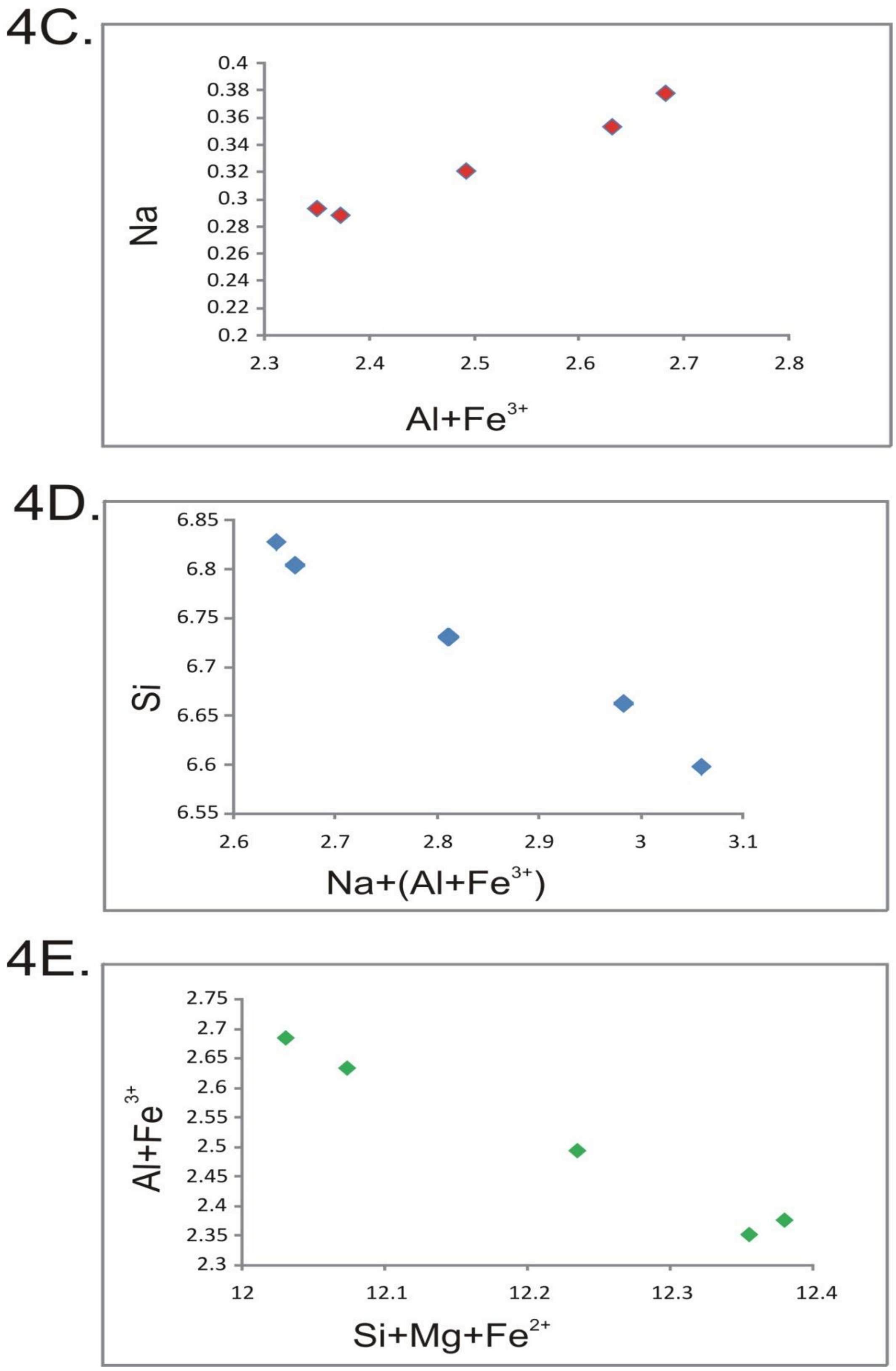

Fig 4C,4D and 4E : Compositional diagrams showing relative variation of gedrite composition.

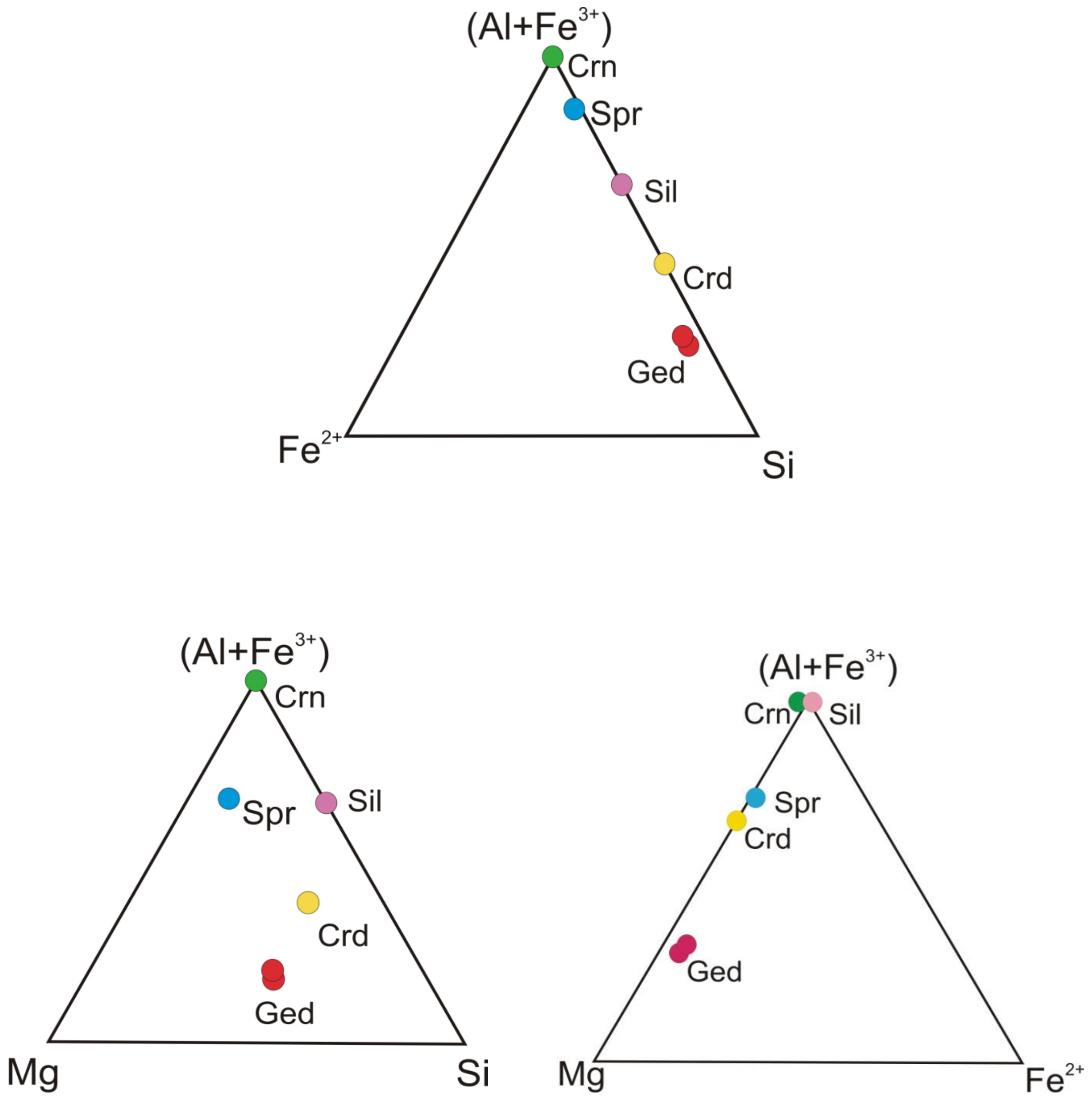

Fig 4F: Chemographic FAS, MAS and AFM diagram representing mineral composition of sapphirine, cordierite, corundum, sillimanite and gedrite (projected from H_2O).

5. Textural modeling with algebraic analysis:

5.1 Mineral evolution:

Textural features suggest gedrite, sillimanite and rutile were the primary minerals present in the rock. Due to the absence of any precursor minerals included within this assemblage (except inclusion of quartz within gedrite), the evolution of this assemblage cannot be determined with certainty. However, presence of distinct disequilibrium textures (like corona) preserved in the micro domains provides important information about the retrogression reactions.

As the sillimanite and the gedrite are never in contact with each other and always separated by double corona of cordierite and cordierite + sillimanite symplectite, it indicates the following reaction:

Gedrite + sillimanite = sapphirine + cordierite ……….(1)

Formation of sapphirine + cordierite symplectic corona adjacent to the sillimanite and cordierite corona adjacent to gedrite is a perfect example of how mobility of elements controls mineral growth. Here, immobility of aluminium resulted in the growth of the more aluminous phases (i.e. sapphirine) adjacent to or over its source sillimanite and the less aluminous phases (i.e. cordierite) away from it.

Presence of corundum within small embayment into sillimanite and absence of sapphirine from its adjacent domains indicate corundum formation initiated after the formation of sapphirine by the following reaction:

Sillimanite + Sapphirine = Cordierite + Corundum ……….(2)

For textural modeling, these reactions are balanced with the help of a software named C-Space.

5.2 Theory of C-space modeling :

C-Space is a program for the graphical and algebraic analysis of composition relations within chemical systems. The program is particularly suited to the needs of petrologists, but could also prove useful for mineralogists, geochemists and other environmental scientists. A few examples of what can be accomplished with C-Space are the mapping of compositions into some desired set of system/phase components, the estimation of reaction/mixing coefficients and assessment of phase-rule compatibility relations within or between complex mineral assemblages. The program also allows dynamic inspection of compositional relations by means of barycentric plots. C-Space provides an integrated work-place for data management, manipulation and plotting. Data management is done through a built-in spreadsheet-like editor, which also acts as a data repository for the graphical and algebraic procedures. Algebraic capabilities are provided by a mapping engine and a matrix analysis tool, both of which are based on singular-value decomposition. The mapping engine uses a general approach to linear mapping, capable of handling determined, under determined and over determined problems. The matrix analysis tool is implemented as a task ``wizard" that guides the user through a number of steps to perform matrix approximation (finding nearest rank-deficient models of an input composition matrix), and inspection of null-reaction space relationships (i.e. of implicit linear relations among the elements of the composition matrix). Graphical capabilities are provided by a graph engine that directly links with the contents of the data editor. The graph engine can generate sophisticated 2-D ternary (triangular) and 3D quaternary (tetrahedral) barycentric plots and includes features such as interactive re-sizing and rotation, on the fly coordinate scaling and support for automated drawing of tie lines.

The law of conservation of mass states that the total mass of all substances present before and after a chemical reaction remains the same. That is, atoms are neither created nor destroyed in chemical reaction, so the chemical equations must be balanced. If there are *m* numbers of linear equations connecting *n* number of independent variables then it can the equations can be written as,

$$\begin{array}{c} a_{11}X_1 + a_{12}X_2 + a_{13}X_3 + \ldots + a_{1n}X_n = Y_1 \\ a_{21}X_1 + a_{22}X_2 + a_{23}X_3 + \ldots + a_{2n}X_n = Y_2 \\ a_{31}X_1 + a_{32}X_2 + a_{33}X_3 + \ldots + a_{3n}X_n = Y_3 \\ \ldots\ldots\ldots\ldots\ldots\ldots\ldots\ldots\ldots\ldots\ldots\ldots\ldots\ldots.. \\ a_{m1}X_1 + a_{r2}X_2 + a_{r3}X_3 + \ldots + a_{mn}X_n = Y_m \end{array}$$

This can be written in the matrix form as, A.X= Y,…….(1)

$$\begin{pmatrix} a11 & a12 & a13 & \ldots & a1n \\ a21 & a22 & a23 & \ldots & a2n \\ \ldots & \ldots & \ldots & \ldots & \ldots \\ am1 & am2 & am3 & & amn \end{pmatrix} . \begin{pmatrix} X1 \\ X2 \\ \ldots \\ Xn \end{pmatrix} = \begin{pmatrix} Y1 \\ Y2 \\ \ldots \\ Yn \end{pmatrix}$$

Where A is a*m* by *n* matrix describing the *m* number of phases with *n* number of system components which are variables. There exists a number of techniques e.g. Gauss Jordon elimination, SVD etc. to solve the equation (1) (Press et al. 1989). C-Space uses singular value decomposition (SVD) which was first introduced to petrologic applications by Fisher (1989; see this paper for a discussion of the relative merits of SVD with regard to other algebraic techniques). SVD encompasses a most useful family of methods in linear algebra which derives from a theorem that states that any m by n matrix A (m > =n) can be written as the product of an *m* by *r* column-orthogonal matrix U, an *r* by *r* diagonal matrix Σ with positive or zero elements, and the transpose of an *n* by *r* orthogonal matrix V:

$$\mathbf{A = U\,\Sigma\,V^t}$$

The usefulness of SVD derives from several of its fundamental properties. The SVD of a matrix can always be obtained, whether it is singular or not, and is almost unique (up to same permutations of columns of U, Σ and V, or linear combinations of U and V columns with equal corresponding elements of Σ). Both U and V are orthogonal, so their inverse is simply their transpose (i.e., $U^t U = V^t V = I$, the identity matrix). The number of non-zero diagonal elements of Σ (called singular values) gives the rank of A, whereas U and V each contain a set of independent vectors (also called ``orthonormal basis") that fully characterize the range and null space of A, respectively. Of particular interest is that the columns of V whose same-numbered elements of Σ are zero form an orthonormal basis for the null space, thus directly giving coefficients for any linear dependencies in A. These, or any linear combination thereof, fully represent the range of linear relations (such as reactions or mass-balances) implicit in a matrix of compositions. A major advantage of SVD is that it allows robust handling of linear systems of equations such as Eq. (1) because of its ability to diagnose problems when the matrix of compositions A is nearly singular through simple inspection of its singular values. The mathematics and computation of SVD are discussed by, e.g., Golub and Van Loan (1983) and Press et al. (1989).

Now *m* numbers of phases are taken in the rows and *n* numbers of components are taken in the columns in the C-Space data window to generate *m* by *n* matrix of A. The Matrix Analyze Wizard (MAW) helps to derive every possible reaction based on the phase component relationships. Out of the possible balanced reaction only those which can explain the textural and mineral assemblages are considered. C-Space's graph window is also helpful of generating triangular and 3D single and stereoscopic tetrahedral barycentric plots where tieline flip reactions and compositions of different minerals has been plotted. The C-Space programme, which is based on the algorithm published by Fisher (1989, 1993) is, therefore, an elegant tool to model reaction textures that may help decipher the physico-chemical conditions, which a given rock might have evolved through (Lang et al. 2004, Sengupta et al. 2009).

5.3 Textural modeling with the help of C-Space programme:

With the help of the C-space programme, the measured compositions of gedrite, sillimanite, sapphirine, cordierite, corundum are plotted on NMAS tetrahedral volume (Fig.5). This chemographic projection shows distinct 'tieline flip' relation relations between the phases which corroborates well with the reaction 1 and 2 predicted from textural observations.

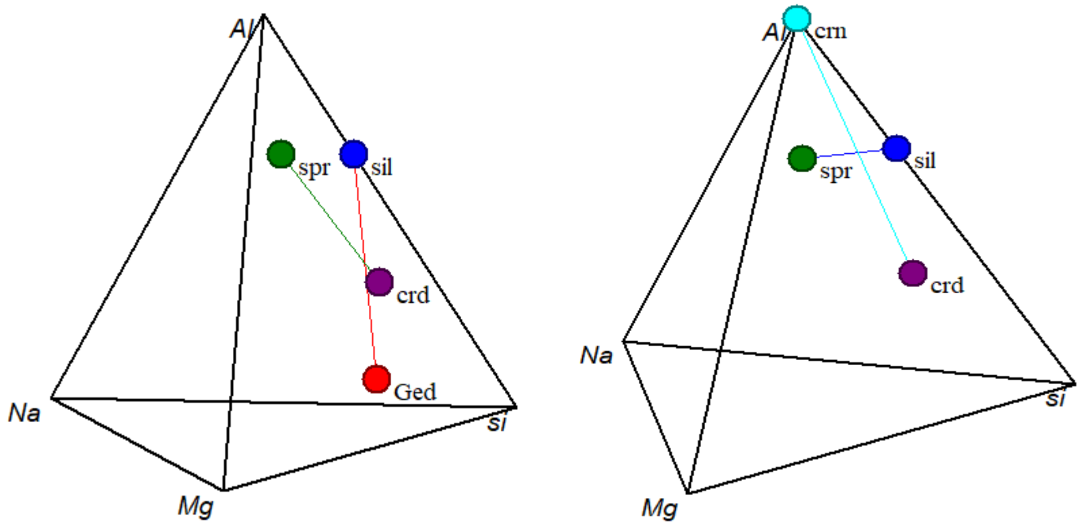

Fig-5: Chemographic diagram showing compositions of the studied minerals in NMAS volume projected from H_2O. The compositions suggest the following tieline flip reaction 1) Gedrite + Sillimanite = Sapphirine + Cordierite 2) Sillimanite + Sapphirine = Cordierite +Corundum.

Algebraic analysis of mineral compositions is a powerful tool to obtain balanced chemical reactions that explain the mineralogy and texture of the rocks formed in open or close systems (Fisher 1989; Lang et al. 2004). Singular value decomposition (SVD) is a simple but robust technique that is widely used by the geoscientists for modeling metamorphic textures (Lang and Rice 1985; Lang et al. 2004; Chowdhury et al. 2013 and the references cited there in). This technique checks linear dependencies and suggests possible reactions from a compositional matrix M of m minerals in terms of n components (Lang et al. 2004). In this study, the computer program C-Space (Torres-Roldan et al. 2000) was used to perform the matrix operation required for SVD. The chemical species whose compositions are suspected to have changed during the reactions are considered as mobile components during matrix operation. The mineral compositions that are used for the matrix analyses are indicated by asterisk mark in the compositional tables.

For the studied rock a total of 10 (m) minerals and mobile phases (6 immobile & 4 mobile) are chosen whose compositions are defined by 7 (n) system components. The C-Space program returns several balanced chemical reactions solving the m × n matrix.

Of the probable reactions, those that satisfy the following criteria are likely to explain the formation of the sapphirine-cordierite coronal textures (reaction 1 predicted from petrographic study) in the studied rocks:

i) The reactant and product phases as deduced from the textures must fall on the opposite sides of the reaction(s).

ii) The volume of cordierite should be greater than the volume of sapphirine.

iii) The volumes of sillimanite and sapphirine-cordierite symplectite in the deduced reactions must be similar i.e. $\Delta V_{(spr+crd)symp - sill}$ must be ~ 0. This is an essential criterion for pseudomorphism (e.g., Putnis 2002). Based on the textural observation it is assumed that ~1/3rd of the total cordierite constitute the volume of the symplectic cordierite.

Among the reactions predicted by C-Space, the corundum forming reaction that satisfies the following criteria are likely to explain formation of corundum (reaction 2 predicted from petrographic study) in the studied rock:

i) The reactant and product phases as deduced from the textures must fall on the opposite sides of the reaction(s).
ii) The volume ratio of corundum and the reactant sapphirine should be between 1:1 to 1:5.

Using the aforesaid textural criteria as filters the following balanced reactions are obtained:

(1) 5.80 Gedrite + 30.69 Sillimanite + 3.32 Mg^{2+} = 2.05 Sapphirine + 13.66 Cordierite + 1.00 Na^{+} + 2.30 Fe^{2+} + 5.80 H_2O

($\Delta V_{(spr+crd)symp\ -\ sill} = 0.34$)

(2) 130.09 Sillimanite + 12.38 Sapphirine + 1.00 Na^{+}+ = 147.30 Corundum + 20.00 Cordierite + 48.09 SiO_2 + 1.09 Fe^{2+}

($V_{Crn} : V_{Spr} = 1: 1.54$)

The balanced chemical reactions that are presented above provide valuable information about the chemical environments that led to the growth of sapphirine, cordierite and corundum in the studied granulite sample. Requirement of mobile elements to balance reactions indicates that the system was open during their formation and growth. Influx of Mg to the system initiated reaction 1 while Na and Fe were removed from the system. It is possible that part of that Na was used up by reaction 2 during the formation of corundum-cordierite. During this reaction, silica and Fe were removed from the system. Hence fluid infiltration driven metamorphism was responsible for the formation of corundum-sapphirine-cordierite rich assemblage within the orthoamphibolite rock.

6. P-T conditions of formation of the mineral assemblages:

To constrain the P-T conditions of formation of the previously discussed reaction textures, petrogenetic P-T grids have been constructed with the help of PERPLE_X program (version 6.8.6; Connoly; 2005) using the internally consistent thermodynamic data set of Holland & Powell (1998). A simple four component system (MASH: MgO, Al_2O_3, SiO_2, H_2O) with seven pure phases gedrite, sillimanite, cordierite, sapphirine, corundum, quartz and water is chosen. According to the Phase rule, in such a system, each of the invariant point should contain six phases with one phases being absent in each of the invariant points.

Figure.6 shows the P-T grid of the MASH system calculated over a temperature range of 600-1200°C and a pressure range of 4 to 16 kbar, which depicts the general stability field of amphibolite-granulite grade crustal rocks.

Following inferences can be drawn from this P-T topology (Fig. 6).

a) Within this P-T limit, two invariant points viz. [Qtz] and [Crn] are stable.
b) Stability of gedrite + sillimanite increases with pressure.
c) Sapphirine + quartz is stable at >900°C and >8.5 kbar.
d) Stability of cordierite increases towards higher pressure with increasing temperature. Corundum + cordierite is stable in lower pressure part of the stability field of sapphirine + cordierite.

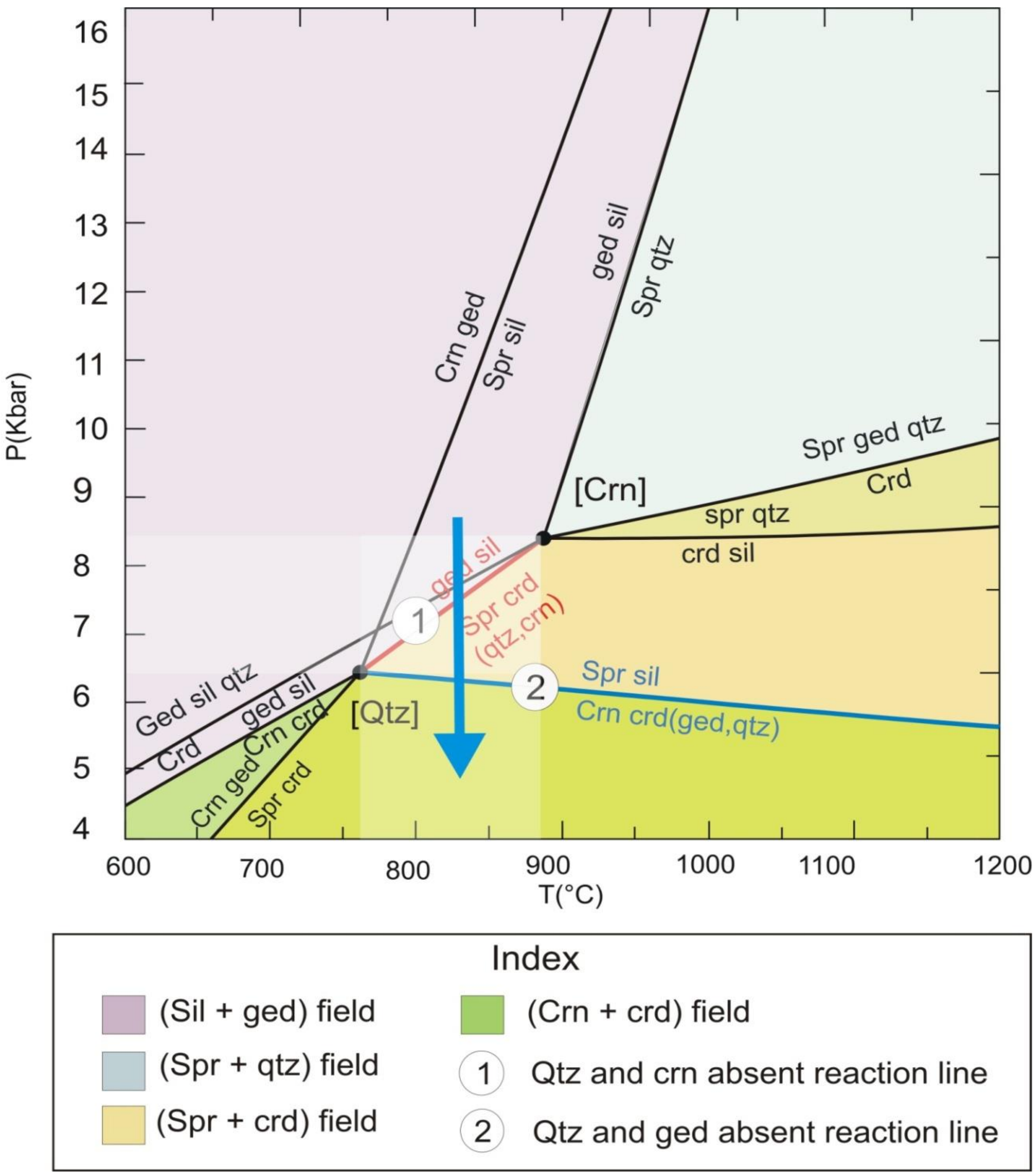

Fig 6: Petrogenetic grid calculated in MASH (MgO, Al_2O_3, SiO_2, H_2O) system with the help of PERPLE_X software Showing stability field of different assemblages (marked by different colours). Reaction 1 & 2 represents the identified reactions obtained from the petrographic study and compositional modeling of the studied rock.

Complete absence of quartz from the sapphirine-cordierite-corundum bearing microdomains of the studied rocks indicates that the assemblage must be associated with [Qtz] invariant point. The (Crn, Qtz) and (Ged, Qtz) univariant lines emerging from the [Qtz] invariant points in Fig. 6 represent the reaction1 and reaction2 respectively, that have been inferred from the microtextural study and chemical analyses. (Crn, Qtz) i.e reaction 1 is bounded by the two invariant points [Qtz] and [Crn] and thus constrains the P-T stability of this reaction within 760-880°C and 6.5-8.5 kbar. Formation of corundum-cordierite through reaction 2 requires crosscutting of the (Ged) univariant line. Hence a steep decompressive path from gedrite-sillimanite stability field that successively passes through sapphirine-cordierite and corundum-cordierite field can explain the formation of the studied assemblages (Fig. 6).

Conclusion:

It is evident from the foregoing discussion that the formation of sapphirine-cordierite-corundum assemblage in the studied rock involves a two-stage reaction process. First, sillimanite-gedrite, the primary minerals of the rock reacted to form sapphirine-cordierite. Immobility of aluminium plays the major role in formation of sapphirine-cordierite symplectic corona or pseudomorph over sillimanite while cordierite forms a collar around it that shared boundary with gedrite. In the second stage, the newly-formed sapphirine reacted with sillimanite to form corundum-cordierite locally along the boundary of sillimanite. Textural modeling through algebraic analysis (SVD technique) shows that several chemical species became mobile during progression of these reactions. The infiltrating fluid that was Mg-rich, exchanged Fe and removed silica from the rock. Na was mobile possibly in local scale. Both experimental and natural studies showed that brine-rich aqueous fluid is an efficient transporter of elements (Newton & Manning 2010). Hence interaction of the rock with externally derived Mg-rich brine is a potential mechanism that initiated the reactions which subsequently led to desilication of the rock. Experimental studies show that silica in aqueous fluid form complex polymers that enhance the element transport and mobility in deep-crustal rocks (Manning 2004). This silica-rich fluid possibly facilitated the removal of different mobile elements from the system.

Petrogenetic grid constrains a decompressive P-T path from 760-880°C and 6.5-8.5 kbar that was responsible for the formation of the studied assemblage. Santosh et al., 2006 constrained the timing of this metamorphism at ~600-500 Ma from similar rocks in adjacent area. Hence our study suggests that during the Pan-African time, at least a part of the CSS underwent exhumation along a steep P-T path in granulite grade conditions. Infiltration of brine-rich fluid during this exhumation led to formation of the corundum-sapphirine-cordierite rich assemblage within the orthoamphibolite rock. This study contradicts with the work by Shimpo et. al. 2006 who proposed UHT conditions was necessary for the stability of corundum-sapphirine-cordierite in parts of the CSS.

Acknowledgement

It is a matter of great pleasure for me to offer my sincere gratitude and cordial thanks to all the persons whose immense help has made this learning experience truly impounding. I am thankful to Department of Geological sciences, Jadavpur University for providing all possible co-operation and necessary infrastructural facilities.

First of all I want to express my heartfelt thanks and deepest regards to Prof. Subrata Karmakar, Department of Geological Sciences, Jadavpur University, under whose guidance this thesis work has been carried out. His kind supervision, valuable guidance, co-operation, suggestion and discussion at every stage have made this thesis work possible.

I also want to express my thanks and deepest regards to Prof. Pulak Sengupta and Prof. Sanjoy Sanyal, Department of Geological Sciences, Jadavpur University, for their expert advice and encouragement throughout this project.

I would really like to take this opportunity to express my heartiest gratitude to Dr. Anindita Dey for her unconditional help and kind suggestions.

I would also like to extend my thanks to Dr. Shreya Karmakar, Dr. Subham Mukherjee, Enakshi Das, Satabdi Das, Nibedita Lahiri, Sirina Roy Choudhury, Arimita chakrabarty and Somdipta Chatterjee for their kind help and co-operation, without them the dissertation would have been incomplete.

Arnab, Swagata both are my batch mates and lab mates helped a lot in the laboratory works for which I am sincerely thankful to them.

Referrences :

Ague, J.J, 2011 Extreme channelization of fluid and the problem of element mobility during Barrovian metamorphism; *Volume 96, pages 333–352.*

Armbruster, T. & Bloss, F.D. 1982. Orientation and effects of channel H2O and CO2 in cordierite. American Mineralogist, 67, 284–291.

Ashworth, J.R. and Birdi, J.J. (1990) Diffusion modelling of coronas around olivine in an open system. Geochimica et Cosmochimica Cosmochimica Acta, 54, 2389–2401.

Braun, I., Kriegsman, L.M., 2003. Proteroozoic crustal evolution of southernmost India and Sri Lanka. In: Yoshida, M., Windley, B.F., Dasgupta, S. (Eds.), Proterozoic East Gondwana: Supercontinent Assembly and BreakupGeol Soc. London, Sp. Publ., vol. 206, pp. 169–202.

Bartlett, J.M.,Dougherty-Page, J.S., Harris, N.B.W., Hawkesworth, C.J., Santosh, M., 1998. The application of single zircon evaporation and Nd model ages to the interpretation of polymetamorphic terrains: an example from the Proterozoic mobile belt of south India. Contrib. Mineral. Petrol. 131, 181–195.

Brown, M., Raith, M., 1996. First evidence of ultrahigh-temperature decompression from the granulite province of southern India. J. Geol. Soc. (Lond.) 153, 819–822.

Chinner, G.A. & Fox, J.S., 1974. The origin of cordieriteanthophyllite rocks in the Land_s End aureole. Geological Magazine, 111, 397–408.
.

Chowdhury, P., Talukdar, M., Sengupta, P., Sanyal, S. & Mukhopadhyay, D. (2013). Controls of P–T path and element mobility on the formation of corundum pseudomorphs in Paleoproterozoic high-pressure anorthosite fromSittampundi, Tamil Nadu, India.American Mineralogist 98, 1725–1737

Chowdhury, P., Gerya, T., & Chakraborty, S. (2016, December). Transition in the mode of syn-collisional continental-recycling with secular cooling of the earth and its implications for crustal evolution. In *AGU Fall Meeting Abstracts*.

Connolly, J. A. D. (2005). Computation of phase equilibria by linear programming: a tool for geodynamic modeling and its application to subduction zone decarbonation. Earth and Planetary Science Letters 236, 524–541.

Diener, J.F.A., Powell, R. & White, R.W., 2008. Quantitative phase petrology of cordierite-orthoamphibole gneisses and related rocks. Journal of Metamorphic Geology, 26, 795–814.

Dutta, U., Bhui, U. K., Sengupta, P., Sanyal, S. & Mukhopadhyay, D. (2011). Magmatic and metamorphic imprints in 2_9Ga chromitites from the Sittampundi layered complex, Tamil Nadu, India. Ore Geology Reviews 40, 90–107.

Das, E., Karmakar, S., Dey, A., Karmakar, S., & Sengupta, P. (2017). Reaction textures, pressure–temperature paths and chemical dates of monazite from a new suite of sapphirine–spinel granulites from parts of the Eastern Ghats Province, India: insights into the final amalgamation of India and East Antarctica during the formation of Rodinia. *Geological Society, London, Special Publications*, *457*(1), 141-170.

Eskola, P., 1914. On the petrology of the Orija¨ rvi region in southwestern Finland. Bulletin of the Geological Commission of Finland, 40, 277.

Fisher, G.W., 1993. An improved method for algebraic analysis of metamorphic mineral assemblages. American Mineralogist 78, 1257±1261.

Ghosh, J.G., de Wit, M.J., Zartman, R.E., 2004. Age and tectonic evolution of Neoproterozoic ductile shear zones in the southern Granulite Terrane of India, with implications for Gondwana studies. Tectonics 23, TC3006. doi:10.1029/2002TC001444.

Golub, G.H., Van Loan, C.F., 1983. Matrix Computations. John Hopkins University Press, Baltimore, 476 pp.

Grew, E.S., 1984. Note on sapphirine and sillimanite+orthopyroxene from Panrimalai, Madurai district, Tamil Nadu. J. Geol. Soc. India 25, 116–119.

Harris, N.B.W., Santosh, M., Taylor, P.N., 1994. Crustal evolution in southern India: constraints from Nd isotopes. J. Geol. 102, 139–150.

Holland, T. J. B. & Powell, R. (1998). An internally consistent thermodynamic data set for phases of petrological interest. Journal of Metamorphic Geology 16, 309–343 [updated online, 2002].

James, R.S., Grieve, R.A.F. & Pauk, L., 1978. The petrology of cordierite-anthophyllite gneisses and associated mafic and pelitic gneisses at Manitouwadge, Ontario. American Journal of Science, 278, 41–63.

Kelsey, D.E., White, R.W. & Powell, R., 2005. Calculated phase equilibria in K2O-FeO-MgO-Al2O3-SiO2-H2O for silicaundersaturated sapphirine-bearing mineral assemblages. Journal of Metamorphic Geology, 23, 217–239.

Koshimoto, K., Tsunogae, T., Santosh, M., 2004. Sapphirine and corundum bearing ultrahigh temperature rocks from the northern domain of Palghat–Cauvery Shear System, Southern India. J. Mineral. Petrol. Sci. 99, 298–310.

Kretz, R. 1983. Symbols for rock-forming minerals. American Mineralogist, 68, 277–279.

Meißner, B., Deters, P., Srikantappa, C. & Ko¨ hler, H. (2002). Geochronological evolution of the Moyar, Bhavani and Palghat shear zones of southern India: implications for east Gondwana correlations. Precambrian Research 114, 149–175.

Newton, R.C. and Manning, C.E. (2010) Role of saline fluids in deep–crustal and upper–mantle metasomatism: insights from experimental studies. Geofluids, 10, 58–72.

Phillpotts, A. & Ague, J. (2009). Principles of Igneous and Metamorphic Petrology. Cambridge: Cambridge University Press.

Plavsa, D., Collins, A. S., Foden, J. F., Kropinski, L., Santosh, M., Chetty, T. R. K. & Clark, C. (2012). Delineating crustal domains in Peninsular India: age and chemistry of orthopyroxene-bearing felsic gneisses in the Madurai Block. Precambrian Research 198–199, 77–93.

Press, W.H., Flannery, B.P., Teukolsky, S.A., Vetterling, W.T., 1989. Numerical Recipes: The Art of Scienti®c Computing. Cambridge University Press, Cambridge, 759 pp.

Putnis, A; (2002); mineral replacement reactions: from Macroscopic Observations to Microscopic Mechanisms.

Putnis, A; (2005); Directed observations of pseudomorphism: compositional and textural evolution at a fluid-solid interface.

Raith, M., Karmakar, S. & Brown, M., 1997. Ultra-hightemperature metamorphism and multistage decompressional evolution of sapphirine granulites from the Palni Hill Ranges, southern India. Journal of Metamorphic Geology, 15, 379–399.

Raith, M.M., Rakotondrazafy, R. & Sengupta, P., 2008. Petrology of corundum-spinel-sapphirine-anorthite rocks (sakenites) from the type locality in southern Madagascar. Journal of Metamorphic Geology, 26, 647–667.

Robinson, P. & Jaffe, H.W., 1969. Aluminous enclaves in gedrite–cordierite gneiss from southwestern New Hampshire. American Journal of Science, 267, 389–421.

Robinson, P., Spear, F.S. & Schumacher, J.C., 1982. Phase relations of metamorphic amphiboles: natural occurrence and theory. In: Reviews in Mineralogy, Vol. 9B (eds Veblen, D. & Ribbe, P.), pp. 1–211. Mineralogical Society of America, Washington, D.C.

Sajeev, K., Osanai, Y., Santosh, M., 2004. Ultrahigh-temperature metamorphism followed by two-stage decompression of garnet– orthopyroxene–sillimanite granulites from Ganguvarpatti Madurai block, southern India. Contrib. Mineral. Petrol. 148, 29–46.

Santosh, M. and Sajeev, K. (2006) Anticlockwise evolution of ultrahigh– temperature granulites within continental collision zone in southern India. Lithos, 92, 447–464.

Shimpo, M., Tsunogae, T., Santosh, M., 2006. First report of garnetcorundum rocks from southern India: implications for prograde high-pressure (eclogite facies?) metamorphism. Earth Planet. Sci. Lett. 242, 111–129.

Schneiderman, J. & Tracy, R.J., 1991. Petrology of orthoamphibole- cordierite gneisses from the Orija¨ rvi area, southwest Finland. American Mineralogist, 76, 942–955.

Schumacher, J.C. & Robinson, P., 1987. Mineral chemistry and metasomatic growth of aluminous enclaves in gedrite– cordierite gneiss from southwestern New Hampshire, USA. Journal of Petrology, 28, 1033–1073.

Schumacher, J.C., 1988. Stratigraphy and geochemistry of the Ammonoosuc Volcanics, central Massachusetts and southwestern New Hampshire. American Journal of Science, 288, 619–663.

Tamashiro, I., Santosh, M., Sajeev, K., Morimoto, T., Tsunogae, T., 2004. Multistage orthopyroxene formation in ultrahigh-temperature granulites of Ganguvarpatti, southern India: implications for complex metamorphic evolution during Gondwana assembly. J. Mineral. Petrol. Sci. 99, 279–297.

Tilley, C.E., 1937. Anthophyllite-cordierite granulites of the Lizard. Geological Magazine, 74, 300–309.

Tsunogae, T., Santosh, M.,2003 Sapphirine and corundum-bearing granulites from Karur, Madurai Block, southern India, Gondwana Res. 6. 925– 930.

Yellappa, T., Santosh, M., Chetty, T. R. K., Kwon, S., Park, C., Nagesh, P., Mohanty, D. P. & Venkatasivappa, V. (2012). A Neoarchean dismembered ophiolite complex from southern India: Geochemical and geochronological constraints on its suprasubduction origin. Gondwana Research 21, 246–265.

Vallance, T.G., 1967. Mafic rock alteration and isochemical development of some cordierite–anthophyllite rocks. Journal of Petrology, 8, 84–96.